Frontiers in Advanced Materials Research

Theoretical Charge density Proof of N–N weak bonds of RDX Energetic Molecule

A. David Stephen [a,*], M. Shankar [a]

[a] Department of Physics, Sri Shakthi Institute of Engineering and Technology, Coimbatore 641 062, India

*Corresponding Author
davidstephen@siet.ac.in
(David Stephen A)

ABSTRACT: The bond topological analysis of Cyclotrimethylene-trinitramine (RDX) energetic molecule has been carried out for the wave function obtained from the *ab initio* and *DFT* methods of quantum chemical calculations. The geometrical parameters of all bonds are compared with that of experimental reports. The inclusion of diffuse function in HF basis set levels makes the significant shift of bond critical point towards carbon atoms of C–N bonds. The heteroatomic bond density character is well understood from unequal C-cp and cp-N distances in all C–N bonds. For all the level of calculations, the maximum bond density was found for all N=O bonds, attributes the maximum potential energy V(r). The N–N bond properties are strongly depends upon the equilibrium bond length which clears from charge concentration in shorter N1–N4 bond and charge depletion found in longer N2–N5 and N3–N6 bonding regions. The bond topological analysis of all bonds in RDX molecule resulted that the N–N bond is the weakest among all the other bonds. The weakness of N2–N5 and N3–N6 bonds than N1–N4 bond of RDX has also been analyzed from energy density calculation from various level of theories as an alternate for Laplacian of electron density. From the analysis of CHELPG charges at the MP2 level, the N–N bonds of RDX appears to have a significant ionic nature which attributes strong hyperconjugation effect. The hyperconjugation effect of RDX, due to polarization of N–N bonds, is the additional proof of weak N–N bonds in RDX explosive. The isosurface electrostatic potential shows the electro positive and negative region in the molecule. A large negative potential found at the vicinity of oxygen atoms.

Keywords: RDX, Quantum Calculation, Electron density, Electrostatic potential, Impact Sensitivity

1. Introduction

To serve fuels or explosives, there has been an extensive search for new high energy density materials (HEDM) for the last couple of decades [1]. Good HEDMs have high density, a fast velocity of detonation (D), which are energetically unstable with respect to their reaction products. The characteristics of such energetic materials depend on various electronic and chemical properties at the molecular level. Such system includes solids, liquids, and gases. Here our studies on RDX are limited to gas phase systems, and primarily consider the electronic properties. For the design of high performance explosives, the analysis of geometry and electronic charge distribution of molecules via theoretical modeling is prerequisite. Several reports [2] includes the characterization of molecules has been carried out using semi-empirical continnum models and further a DFT model also used for these analysis. Therefore, it is important to make a note about the application of electronic and structural parameters in designing the high energetic molecules. The

energetic character based on charge density was investigated by Coffey [3] and Kunz and Beck [4]. The Coffey model is fair less specific in providing the precise physical effects of such regions on the molecules constituting the solid. In addition to the incompleteness of the Coffey model, this theory does not provide a convincing model for the presence of the charges found in the fractoemmision from energetics. Some studies performed by Kunz and Beck provide strong evidence that the presence of charges inside an energetic solid can provide significant diminution of the strength of molecular bonds, and in some instances even cause their dissociation.
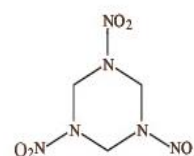
Scheme 1. hexahydro-1,3,5-trinitro-1,3,5-triazine

Compounds that contain polynitro groups are always highly energetic. They can provide a large amount of energy and heat after they are burnt and are employed extensively as the main ingredient in explosives. Nitramines have long been used for technological as well as military purposes[5-9]. It is able to withstand much larger mechanical and thermal shocks without igniting. These characteristics make the material particularly well-suited to a variety of defence and civilian applications.[10,11] To this end, it is very important to investigate one of the common very sensitive explosives, RDX (hexahydro-1,3,5-trinitro-1,3,5-triazine) (scheme 1), which is the energetic polynitro compound. In this article, we present a theoretical investigation of RDX. In the attempt to have a better characterization of the geometric parameters, bond topology of RDX, in the present study, we report the results of *ab initio* calculations [12] at Hartree-Fock(HF) and second-order Moller-Plesset (MP2) levels using different types of basis sets. For the purpose of comparison and as an alternative to the computationally demanding MP2 methods we have also used density functional theory (DFT), in the Kohn-Sham formulation.[13,14] The major aim of the this work is to provide some insight to understanding the strength of various types of bonds and the energy density distribution of the RDX molecule using AIM theory [15]. Hence, the quantum chemical approaches at various level of sophistication coupled with AIM theory allows to characterize the weak and strong bonds, and helpful to predict the bond break in the molecule while it undergoes decomposition. RDX is a nitramine type highly important explosive [6-8]. In practice, usually new energetic materials are designed by modifying known substances by addition and/or modification of energetic group(s) in the molecules.

The theory of atoms in molecules (AIM) [15] calculations were also performed, which permits the investigation of chemical systems on a common basis, as the theory uses only information contained in the electron density $\rho(r)$. The critical points (CP) in the electron density and the Laplacian are the points where $\nabla\rho(r)$ vanish. The topology of the Lapalcian field allows one to recover the chemical model of localized bonded and non-bonded pairs and to characterize local concentrations $\nabla^2\rho(r) < 0$, and depletions, $\nabla^2\rho(r) > 0$, of the electronic charge density distribution. Bader's theory of Atoms[16] in molecules is the theory of chemical structure and reactivity based on the topological properties of the electronic charge density ρ, the formation of the chemical bond is the result of a competition between the perpendicular contractions of ρ towards the bond path, which lead to a concentration of the charge density along this line and parallel expansion of ρ away from the interatomic surface, which leads to separate concentration in each atomic basin. This behavior results in the formation of a critical point in the charge density at which the Hessian of ρ has two negative eigen values (λ_1 and λ_2) and one positive eigen value (λ_3). This means that ρ exhibits two negative curvatures (λ_1 and λ_2)

perpendicular to the interatomic line and one positive curvature (λ_3) along the interaction line. In this theory, the atomic interactions are classified between two limiting behaviors: the *open* and *closed-shell* interactions. The *open-shell* interactions are characteristics of covalent and polar bonds. In this limiting situation, the charge distribution at the BCP is dominated by the perpendicular negative curvature of the electron density. These *open-shell* interactions are characterized [17] by large values of ρ, $\nabla^2\rho(r) < 0$, and $|\lambda_1|/\lambda_3 > 1$ at the BCP. In contrast, for the *closed shell* interactions, characteristics of ionic bonds, hydrogen bonds, and van der Waals molecules, the value of ρ is small, $\nabla^2\rho(r) > 0$ and $|\lambda_1|/\lambda_3 << 1$. These behaviors can be better understood, if we recall that the local form of the virial theorem [18] can be written as

$$(\hbar^2/4m) \nabla^2\rho = 2G(r) + V(r)$$

where $G(r) > 0$ is the electronic kinetic energy density and $V(r) < 0$ is the electronic potential energy density, defined as the virial of the forces exerted on the electrons. Thus the sign of the $\nabla^2\rho$ serves to summarize the essential physical characteristics of the interactions, which create the BCP. For the *closed-shell* interactions the kinetic energy density is dominant contribution at the BCP, while for the *open-shell* interactions the potential energy density makes the prevailing contribution.

2. Computational Details

The geometry optimization of RDX molecule leading to energy minima were achieved by using quantum chemical calculations including *ab initio* and Density functional methods (DFT) and these calculations were performed using the GAUSSIAN03 program.[19] *Ab initio* calculations includes Hartree-Fock (HF) [20] with the basis sets 6-311G** and 6-311++G**. To overcome the electron correlation effects second order Moller-Plesset (MP2) [21] with 6-311G** were employed. Further, DFT calculations include B3LYP,[22] BLYP [23] and BP86 [24] with 6-311G** were also performed. The wave functions obtained from the various optimization procedures were used to calculate the topological properties such as electron density, Laplacian of electron density, and ellipticity at the bond critical points by using the Bader's theory of atoms in Molecules (AIM) implemented in AIMPAC software.[25] The atomic charges derived from NPA, MPA and electrostatic potential derived population (CHELPG) different schemes were calculated for each atom. The deformation densities for each bond of the molecule were plotted by using the software *wfn2plots*.[26]

3. Results and Discussion

3.1. Structural Aspects

Fig 1 depicts the atomic numbering scheme of RDX molecule optimized at MP2/6-311G** level. From the immediate look, it is obvious that the six membered ring is not planar, it

exhibits the chair conformation. The nitro groups attached at 3- and 5- positions are inclined at almost the same angle [60.4, 68.3 and 60.2˚] from the plane of three carbon atoms. But the nitro group at 1- position is essentially coplanar [1.7, 3.7 and 0.8˚] with less deviation from the carbon atom plane. The same trend appears in the molecule optimized at all the levels of theories including the electron correlation effect incorporated MP2 and DFT level of theory. The unique configuration of the 1-nitro groups appears to come from the effect of repulsive non-bonded interaction between adjacent nitro groups.
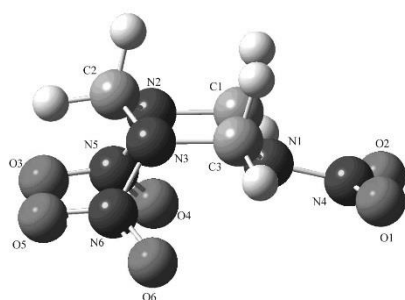

Fig 1. MP2/6-311G** level calculated geometry of RDX with the atomic numbering scheme

As one may notice in Table 1, a controversial geometric feature among the calculation levels is the N1–N4 bond length. Among the N–N bond length, N1–N4 distance is significantly shorter than N2–N5 and N3–N6 distances attributes the repulsive interaction between the nitro groups attached at N2 and N3 atoms. The N1–N4 bond distance calculated from *ab initio* and DF theories are 1.367(HF), 1.416(MP2) and 1.427 Å(DFT) respectively. The N2–N5 [1.382 (HF), 1.440 (MP2), 1.465 Å (DFT)] and N3–N6 [1.381(HF), 1.440(MP2), 1.465Å(DFT)] bonds are 0.015(HF), 0.024(MP2) and 0.013Å (DFT) longer than that of N1–N4 bond. The experimental [27] investigation also reflects the same trend. The N–N bond distances predicted from HF/6-311++G** are found larger, when the electron correlation effect was introduced in the calculation, this distance is further lengthened in DFT level of optimization. The N2–N5 and N3–N6 bond distances predicted for MP2/6-311G** and BP86/6-311G** methods are much longer than experimental [27] crystallographic bond distances [1.392 and 1.398 Å] and are highly overestimated. The differences between the levels are due to the electron correlation and basis set effects. Besides the calculations on N–N bonds, further geometrical calculations also have been made on C–N bonds of RDX. The interesting feature observed in C–N distances for all level of calculations gave the adjacent bond distances in the six-membered ring are equal, and their distances calculated for both *ab initio* and DFT theory are C2–N2=C2–N3: [1.455,

1.461 and 1.467 Å]; C1–N1=C3–N1: [1.466, 1.468 and 1.476 Å] and C1–N2= C3–N3: [1.443, 1.447 and 1.452 Å]. Due to the crystal field effect, this trend is not found in the experimental [27] reported structures as it differ by 0.01 , 0.014 and 0.003 Å respectively. The C–N–C angles of six membered ring are very close except the angle C3–N1–C1 calculated from MP2, which is too narrowed. The average C–N–C bond angles predicted by the methods HF/6-311++G**, MP2/6-311G** and BP86/6-311G** are 114.8, 112.1 and 115.3˚ respectively. Among these angles, the angle from HF well agree with experimental value. The average N–C–N bond angles for the above levels of calculations are 109.6, 110.6 and 110.6˚ respectively, which are found slightly larger than the experimental value 109.3˚. Among these calculations, HF/6-311++G** calculated C–N–C and N–C–N bond angles are almost agrees with the reported experimental average bond angles are 144.8 and 109.3˚ respectively.[27] From, C–N bonds, the maximum bond twist noticed in C1–N1 and C3–N1 bonds. The torsion angles predicted by HF/6-311++G**, MP2/6-311G** and BP86/6-311G** methods for the bonds C1–N1: 167.5, 169.9, 166.3˚ and C3–N1: -167.5, -169.9, -166.3˚ respectively. Also among the N–N bonds, the maximum bond twist was noticed in N2–N5 and N3–N6 bonds. For N2–N5 bond, it is 168.4, 166.5 and 166.3˚ and for N3–N6 bond 158.1, 151.0 and 159.0˚ respectively. The MP2 and DFT values are expected to be same as in HF but here they differ by ~10˚, this unequal twist may be due to the folding of six membered ring as it is differentiated among the different level of calculations. This inequality of conformation is important. The C–N and N–O bonds are *trans* oriented with respect to N–N.

Table I. Important geometric parameters^a of RDX calculated by various levels of theories.

3.2. CHARGE DENSITY AND LAPLACIAN OF ρ

Fig 2, depicts the total electron density in the molecular plane calculated from MP2/6-311G** method. The whole spectrum of bond electron density distribution in the molecule from various levels of quantum chemical calculations are listed in Table 2. The bond density at the critical point ρ_{bcp} of adjacent C–N bonds in the six membered ring are equal. The average values of ρ_{bcp} for C–N bonds predicted by HF, MP2 and DFT methods are ~1.80, ~1.78 and ~1.77 eÅ^{-3} respectively. Specifically, the inclusion of diffuse function in the basis sets of HF calculations made any significant change either in the ρ_{bcp} values or the position of critical points in the bond. The laplacian of C1–N2, C2–N2 and C3–N3 ranges -13.8 to -18.1eÅ^{-5}.

Table I. Important geometric parameters[a] of RDX calculated by various levels of theories.

Bond lengths	HF/6-311++G**	MP2/6-311G**	BP86/6-11G**	Expt.
C1–N1	1.466	1.468	1.476	1.464(4)
C1–N2	1.443	1.447	1.452	1.443(4)
C2–N2	1.455	1.461	1.467	1.468(4)
C2–N3	1.455	1.461	1.467	1.458(4)
C3–N1	1.466	1.468	1.476	1.450(4)
C3–N3	1.443	1.447	1.452	1.440(4)
N1–N4	1.367	1.416	1.427	1.351(3)
N2–N5	1.382	1.44	1.465	1.392(3)
N3–N6	1.381	1.44	1.465	1.398(3)
N4–O1	1.185	1.222	1.231	1.209(5)
N4–O2	1.185	1.222	1.231	1.233(5)
N5–O3	1.181	1.218	1.224	1.203(5)
N5–O4	1.182	1.219	1.225	1.207(5)
N6–O5	1.181	1.218	1.224	1.201(5)
N6–O6	1.182	1.219	1.225	1.205(5)
C1–H1	1.086	1.1	1.108	1.058(10)
C1–H2	1.069	1.084	1.092(8)	1.092(8)
C2–H3	1.071	1.085	1.095	1.085(8)
C2–H4	1.081	1.093	1.102	1.087(7)
C3–H5	1.086	1.1	1.108	1.088(8)
C3–H6	1.069	1.084	1.094	1.075(9)
Bond angle				
N1–C1–N2	108.6	109	109.3	107.8(2)
N1–C1–H1	110.4	111	111.1	109.9(4)
N1–C1–H2	110.2	109.6	109.2	110.0(4)
N2–C1–H1	107.1	106.8	107.6	108.0(4)
N2–C1–H2	110.7	110.2	109.8	110.0(5)
H1–C1–H2	109.8	110.3	109.8	111.0(6)
N2–C2–N3	111.7	113.9	113.4	111.7(2)
N2–C2–H3	110.8	109.8	109.3	110.1(4)
N2–C2–H4	106.7	106.5	107.5	106.9(4)
N3–C2–H3	110.8	109.8	109.3	110.7(4)
N3–C2–H4	106.7	106.5	107.5	107.2(4)
H3–C2–H4	109.9	110.2	109.9	110.1(6)
N1–C3–N3	108.6	109	109.3	108.4(2)
N1–C3–H5	110.4	111	111.1	109.6(4)
N1–C3–H6	110.2	109.6	109.2	111.3(5)
N3–C3–H5	107.1	106.8	107.6	107.4(4)
N3–C3–H6	110.7	110.2	109.8	111.1(4)
H5–C3–H6	109.8	110.3	109.9	108.8(6)
C1–N1–C3	114.3	111.8	114.6	115.1(2)
C1–N1–N4	115.1	113.5	115.6	119.7(2)

C3–N1–N4	115.1	113.5	115.6	120.9(2)
C1–N2–C2	115.1	113.5	115.7	114.6(2)
C1–N2–N5	116.9	113.8	115.7	117.1(2)
C2–N2–N5	117.4	114.6	116.3	116.6(2)
C2–N3–C3	115.1	113.4	115.7	114.8(2)
C2–N3–N6	117.4	114.6	116.3	117.5(2)
C3–N3–N6	116.9	113.8	115.7	115.6(2)
N1–N4=O1	117	116.4	116.3	117.2(3)
N1–N4=O2	117	116.4	116.3	117.8(3)
O1=N4=O2	126	127.1	127.3	125.0(3)
N2–N5=O3	116.5	115.7	115.8	117.2(3)
N2–N5=O4	117.1	116.5	116.3	116.8(3)
O3=N5=O4	126.2	127.6	127.8	125.7(4)
N3–N6=O5	116.5	115.7	115.8	117.3(3)
N3–N6=O6	117.1	116.5	116.3	117.0(3)
O5=N6=O6	126.2	127.6	127.8	125.5(4)
Torsion angles				
N2–C1–N1–C3	-55.9	-60.1	-55.5	-57.4
N2–C1–N1–N4	167.5	169.9	166.3	145.6
H1–C1–N1–C3	61.2	57.2	63.1	60.1
H1–C1–N1–N4	-75.4	-72.7	-75.1	-96.9
H2–C1–N1–C3	-177.3	179.2	-175.6	-177.4
H2–C1–N1–N4	46.1	49.3	46.2	25.6
N1–C1–N2–C2	51.9	52.7	49.3	52.1
N1–C1–N2–N5	-92	-80.7	-91.6	-89.8
H1–C1–N2–C2	-67.4	-67.2	-71.5	-66.6
H1–C1–N2–N5	148.7	159.3	147.7	151.6
H2–C1–N2–C2	173	173	169	172.1
H2–C1–N2–N5	29.1	39.6	28.1	30.2
N3–C2–N2–C1	-49.3	-47.3	-44.9	-49.4
N3–C2–N2–N5	94.4	85.7	95.7	92.6
H3–C2–N2–C1	-173.4	-170.8	-167	-172.9
H3–C2–N2–N5	-29.6	-37.8	-26.4	-30.9
H4–C2–N2–C1	67	69.8	73.7	67.5
H4–C2–N2–N5	-149.3	-157.1	-145.7	-150.4
N2–C2–N3–C3	49.3	47.4	44.9	49.2
N2–C2–N3–N6	-94.4	-85.6	-95.7	-91.9
H3–C2–N3–C3	173.4	170.9	167.1	172.3
H3–C2–N3–N6	29.6	37.9	26.4	31.2
H4–C2–N3–C3	-67	-69.8	-73.7	-67.6
H4–C2–N3–N6	149.3	157.2	145.6	151.3
N3–C3–N1–C1	55.9	60.1	55.5	57.2
N3–C3–N1–N4	-167.5	-169.9	-166.3	-146.1
H5–C3–N1–C1	-61.2	-57.2	-63.1	-59.7

H5–C3–N1–N4	75.4	72.8	75.1	97
H6–C3–N1–C1	177.3	-179.2	175.6	179.8
H6–C3–N1–N4	-46.1	-49.2	-46.2	-23.5
N1–C3–N3–C2	-51.9	-52.8	-49.3	-51.9
N1–C3–N3–N6	92.1	80.6	91.6	89.9
H5–C3–N3–C2	67.4	67.2	71.4	66.4
H5–C3–N3–N6	-148.7	-159.4	-147.6	-151.8
H6–C3–N3–C2	-173	-173.1	-169	-174.7
H6–C3–N3–N6	-29	-39.7	-28.1	-32.9
C1–N1–N4=O1	158.9	155.8	159.9	171.5
C1–N1–N4=O2	-22.5	-26.7	-22.1	-10.1
C3–N1–N4=O1	22.6	26.7	22.1	15.9
C3–N1–N4=O2	-158.8	-155.8	-159.9	-165.8
C1–N2–N5=O3	168.4	166.5	166.3	169
C1–N2–N5=O4	-14.9	-18	-18.3	-16.3
C2–N2–N5=O3	25.3	33.6	25.7	28
C2–N2–N5=O4	-158	-150.9	-159	-157.3
C2–N3–N6=O5	-25.3	-33.5	-25.6	-20.5
C2–N3–N6=O6	158.1	151	159	163.9
C3–N3–N6=O5	-168.4	-166.3	-166.3	-161.3
C3–N3–N6=O6	15	18.2	18.3	23.2

[a]Units are Å for bond lengths and in degrees for bond angles, torsion angles and dihedral angles.
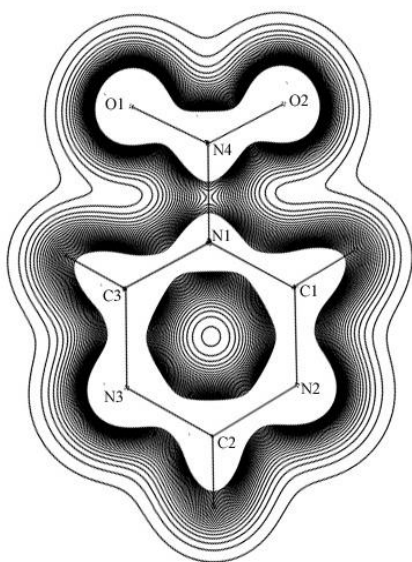

Fig 2. Total density of RDX molecule at molecular plane plotted from MP2/6-311G** level. Contours are drawn at 0.05 eÅ^{-3}.

The critical points in the C–N bonds are off from the middle points, but they shifted towards the C-atoms, which indicates that C–N bond densities are highly polarized to C-atom. This effect is more pronounced on the introduction of polarization function in HF calculation. The C–N bond densities obtained from MP2 and DFT methods are slightly smaller except C3–N3 bond (consistently all methods found higher density) on comparing with HF, the corresponding $\nabla^2\rho_{bcp}(r)$ values, which ranges from -13.8 to -18.1 eÅ^{-5}. Among the DFT calculations, the maximum bond density ρ_{bcp} for all C–N bonds was found in B3LYP/6-311G** level, which was randomly decreased in BLYP and BP86 methods. The unequal C–cp and cp–N distances in all C–N bonds prove the location of the heteroatomic bond density which never lie at the middle of internuclear axis as it is mostly found at the centre in the homo atomic bonds. The charge accumulation in the N=O bonds of three NO_2 groups in the molecule are found to be almost equal, despite, the different basis set levels. However, the charge accumulation in these bonds are found to large in HF model calculation. And the MP2 calculation gave the moderate ρ-values as 3.377 – 3.384 eÅ^{-3} and the average is 3.380 eÅ^{-3}. This value is almost close to the values calculated from DFT level [B3LYP/6-311G**, BP86/6-311G**]. The $\nabla^2\rho_{bcp}(r)$ values for these bonds from MP2 level are -23.5 to -23.9 eÅ^{-5}. These values are slightly lower than B3LYP but higher than BLYP and BP86 level DFT calculation. The CP's in bonds are found shifted towards N-atoms of N–O bonds, indicates the polarization. Fig 3 (a-c), shows the deformation density of N–NO_2 groups in the molecule, and its corresponding Laplacian of density [Fig 3(d-f)] at the bond critical points. Depending upon the method of calculation, the bond properties of N–N bonds varies significantly.
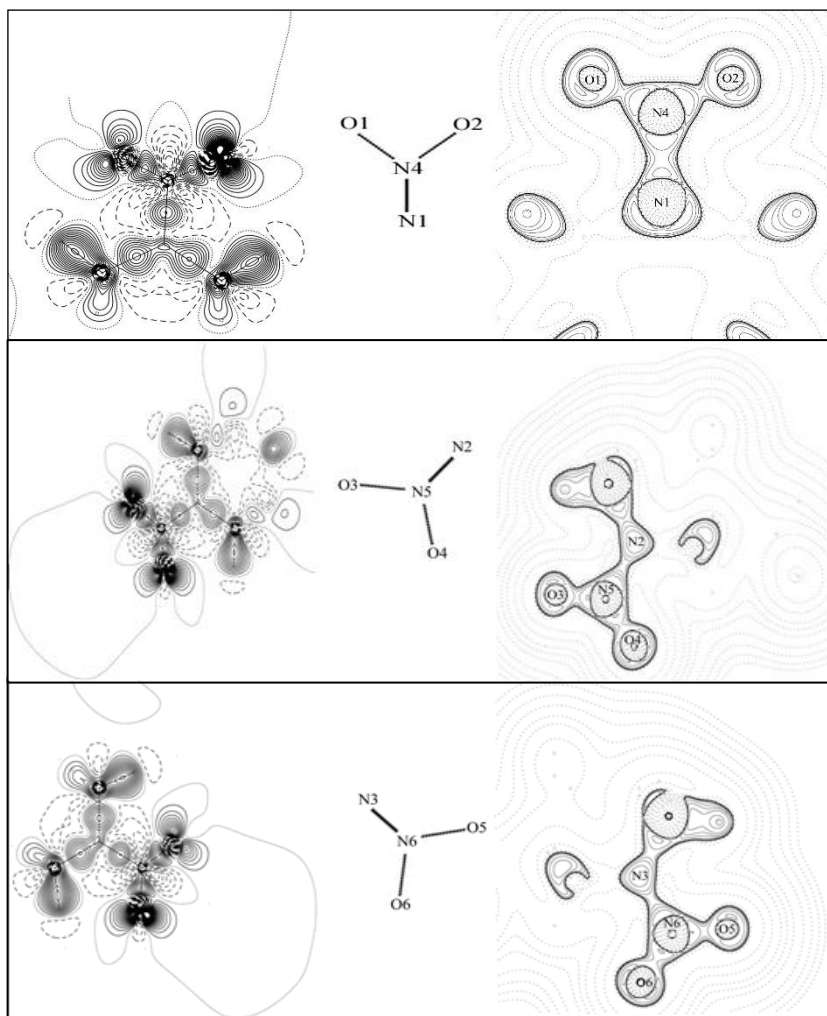
Fig 3. Static deformation density (a-c) and Laplacian (d-f) of N–NO₂ fragments. In the deformation density, the positive contours (solid lines) and negative contours (dashed lines) are drawn at 0.05 eÅ⁻³. In the Laplacian, solid lines shows positive contours and dashed lines are negative contours.

The N–N bond densities in the molecule are expected to equal, but, surprisingly the N1–N4 bond density is larger than N2–N5 and N3–N6 bond densities as they are almost equal. At HF/6-311++G** level, the electron density $\rho_{bcp}(r)$ of N1–N4, N2–N5 and N3–N6 bonds are 2.554, 2.472 and 2.472 eÅ⁻³ respectively. The Laplacian of electron density $\nabla^2\rho_{bcp}(r)$ at the bond critical points of N–N bonds are ˜22.5, ˜20.9 and ˜20.9 eÅ⁻⁵ respectively. The $\rho_{bcp}(r)$ and $\nabla^2\rho_{bcp}(r)$ of N–N bonds are found decreased significantly in the electron correlation method MP2 level and the values for the bonds N1–N4, N2–N5 and N3–N6 are 2.188 eÅ⁻³, ˜12.2 eÅ⁻⁵; 2.08 eÅ⁻³, ˜10.5 eÅ⁻⁵ and 2.08 eÅ⁻³, ˜10.5 eÅ⁻⁵ respectively. These values are found to be small in DF level of calculation. The decrease in density at CP can be clearly confirmed from the less negative value of Laplacian obtained from DFT calculations indicates, the large charge depletion in these bonds and the values are ˜8.31(BLYP), ˜9.5 eÅ⁻⁵ (BP86) for N1–N4 and ˜5.8 (BLYP), ˜7.0 eÅ⁻⁵(BP86) for N2–N5 and N3–N6. The less negative value of Laplacian, indicates the N–N bond charges are largely depleted on comparing all other bonds in the molecule. This confirms that the bonds are very weak. This prediction supports the structural investigation on

RDX molecule.[27] As expected the CP's of the N–N bonds are not at the middle of these bonds, and they are shifted to either sides, the minimum and maximum shift in this bond in HF, MP2 and DFT levels are ranges for N1–N4: 0.072 to 0.024, N2–N5: 0.067 to 0.024 and N3–N6: 0.067 to 0.021 Å. The CP positions of N–N bonds were shifted to middle of the internuclear axis as the density decreases and the bond path length also increased. Based on these results, we conclude that N–N bonds are the weakest bonds among all the bonds in RDX molecule. In the N–N bonds, specifically, the N1–N4 having shorter bond length and exhibit high electron density and high charge concentration. The low electron density and depleted charges were found for N2–N5 and N3–N6 bond having longer bond length. This reveals that, the bond properties strongly depend upon the equilibrium bond length. Fig 4(a-c) depicts the exact variation of $\rho_{bcp}(r)$ and $\nabla^2\rho_{bcp}(r)$ for various bonds of molecule.

The bond ellipticities is the measure of anisotropy of electron density distribution at CP. It can be calculated from the ratio of the negative values of $\varepsilon = (\lambda_1/\lambda_2)$˜1. The Table 2 reveals the whole spectrum of the shape of electron density

distribution at the critical points of bonds in the molecule. The ellipticity values of C3–N1 and C1–N1 bonds are same (0.092) and these values are much greater than the values found in the similar type of bonds C1–N2 and C2–N2; C3–N3 and C2–N3 (ranges 0.052-0.056), these low values of ellipticity in C–N bonds indicate that the bond densities in the bond are slightly distorted. Further, on compared to above values with the N–N bonds (average 0.227) and N=O bonds (average 0.117) are much smaller, attributes different bonding nature and shows the anisotropy in the bond densities. The order of ellipticities of the bonds are C–N < N–N < N=O. The trend in

DFT calculation is C–N < N=O < N–N and in HF also found the same order. On the whole, the ellipticity obtained from correlation functions incorporated in MP2 and DFT calculations are consistently gave smaller values and specifically, the higher level DFT calculations gave still smaller values. This may be attributed to the less screening of bonding electrons in the molecule, hence the bonding densities preserve the isotropicity even though they are depleted. However, the values obtained from the MP2 level are reasonable and are comparable with similar type depleted bonds in the molecule

Tabe II. Bond topological parameters of RDX molecule

Bonds	ρ [eÅ^{-3}]	$\nabla^2\rho$[eÅ^{-5}]	ε	d_1[Å]	d_2[Å]	d[Å]
C1–N1						
HF/6-311G**	1.765	-15.354	0.191	0.495	0.970	1.466
HF/6-311++G**	1.760	-15.332	0.190	0.496	0.971	1.467
MP2/6-311G**	1.751	-16.567	0.092	0.570	0.900	1.469
B3LYP/6-311G**	1.731	-15.721	0.105	0.583	0.890	1.473
BLYP/6-311G**	1.677	-13.785	0.090	0.611	0.876	1.488
BP86/6-311G**	1.709	-14.540	0.092	0.598	0.879	1.477
C2–N2						
HF/6-311G**	1.786	-14.411	0.181	0.487	0.968	1.455
HF/6-311++G**	1.781	-14.371	0.181	0.487	0.969	1.456
MP2/6-311G**	1.764	-16.684	0.056	0.561	0.901	1.463
B3LYP/6-311G**	1.758	-16.098	0.060	0.573	0.890	1.463
BLYP/6-311G**	1.706	-14.246	0.043	0.602	0.875	1.477
BP86/6-311G**	1.732	-14.877	0.047	0.589	0.879	1.468
C3–N3						
HF/6-311G**	1.840	-15.343	0.164	0.483	0.961	1.444
HF/6-311++G**	1.835	-15.276	0.165	0.483	0.961	1.445
MP2/6-311G**	1.825	-18.101	0.052	0.552	0.896	1.448
B3LYP/6-311G**	1.814	-17.400	0.054	0.564	0.885	1.450
BLYP/6-311G**	1.768	-15.675	0.033	0.592	0.870	1.461
BP86/6-311G**	1.789	-16.212	0.039	0.580	0.874	1.454
C1–N2						
HF/6-311G**	1.840	-15.327	0.164	0.483	0.961	1.444
HF/6-311++G**	1.835	-15.276	0.165	0.483	0.961	1.445
MP2/6-311G**	1.825	-18.104	0.052	0.552	0.896	1.448
B3LYP/6-311G**	1.815	-17.403	0.054	0.564	0.885	1.450
BLYP/6-311G**	1.768	-15.675	0.033	0.592	0.870	1.461
BP86/6-311G**	1.790	-16.213	0.039	0.580	0.874	1.454
C2–N3						
HF/6-311G**	1.787	-14.434	0.181	0.487	0.968	1.455
HF/6-311++G**	1.781	-14.369	0.181	0.487	0.969	1.456

MP2/6-311G**	1.764	-16.688	0.056	0.561	0.901	1.463
B3LYP/6-311G**	1.758	-16.100	0.060	0.573	0.890	1.463
BLYP/6-311G**	1.706	-14.247	0.043	0.602	0.875	1.477
BP86/6-311G**	1.732	-14.880	0.047	0.589	0.879	1.468

Bonds	$\rho\,[e\text{Å}^{-3}]$	$\nabla^2\rho\,[e\text{Å}^{-5}]$	ε	$d_1[\text{Å}]$	$d_2[\text{Å}]$	$d[\text{Å}]$
C3–N1						
HF/6-311G**	1.765	-15.349	0.190	0.495	0.970	1.466
HF/6-311++G**	1.760	-15.332	0.190	0.496	0.971	1.467
MP2/6-311G**	1.751	-16.570	0.092	0.570	0.900	1.469
B3LYP/6-311G**	1.731	-15.724	0.105	0.583	0.890	1.473
BLYP/6-311G**	1.677	-13.777	0.090	0.612	0.876	1.488
BP86/6-311G**	1.789	-14.532	0.092	0.598	0.879	1.477
N1–N4						
HF/6-311G**	2.567	-22.856	0.278	0.647	0.719	1.367
HF/6-311++G**	2.554	-22.524	0.276	0.647	0.721	1.368
MP2/6-311G**	2.188	-12.192	0.231	0.695	0.721	1.416
B3LYP/6-311G**	2.243	-12.728	0.252	0.686	0.719	1.405
BLYP/6-311G**	2.024	-8.313	0.237	0.708	0.735	1.443
BP86/6-311G**	2.103	-9.510	0.242	0.702	0.726	1.427
C3–N3						
HF/6-311G**	1.840	-15.343	0.164	0.483	0.961	1.444
HF/6-311++G**	1.835	-15.276	0.165	0.483	0.961	1.445
MP2/6-311G**	1.825	-18.101	0.052	0.552	0.896	1.448
B3LYP/6-311G**	1.814	-17.400	0.054	0.564	0.885	1.450
BLYP/6-311G**	1.768	-15.675	0.033	0.592	0.870	1.461
BP86/6-311G**	1.789	-16.212	0.039	0.580	0.874	1.454
N2–N5						
HF/6-311G**	2.483	-21.229	0.280	0.657	0.724	1.381
HF/6-311++G**	2.472	-20.939	0.278	0.656	0.726	1.382
MP2/6-311G**	2.076	-10.519	0.226	0.709	0.731	1.440
B3LYP/6-311G**	2.093	-10.396	0.246	0.701	0.734	1.435
BLYP/6-311G**	1.837	-5.800	0.232	0.730	0.755	1.486
BP86/6-311G**	1.927	-7.043	0.234	0.721	0.745	1.466
N3-N6						
HF/6-311G**	2.482	-21.214	0.279	0.657	0.724	1.381
HF/6-311++G**	2.472	-20.943	0.278	0.656	0.726	1.382
MP2/6-311G**	2.076	-10.516	0.226	0.709	0.731	1.440
B3LYP/6-311G**	2.092	-10.393	0.246	0.701	0.734	1.435
BLYP/6-311G**	1.837	-5.806	0.232	0.730	0.755	1.486
BP86/6-311G**	1.928	-7.049	0.234	0.721	0.745	1.466
N4-O1						
HF/6-311G**	3.859	-39.417	0.137	0.571	0.613	1.184
HF/6-311++G**	3.848	-39.322	0.137	0.570	0.615	1.185

MP2/6-311G**	3.355	-23.496	0.119	0.580	0.643	1.222
B3LYP/6-311G**	3.420	-24.714	0.106	0.586	0.633	1.219
BLYP/6-311G**	3.235	-19.717	0.093	0.595	0.641	1.237
BP86/6-311G**	3.287	-21.061	0.095	0.590	0.640	1.231

Bonds	ρ [eÅ^{-3}]	$\nabla^2\rho$[eÅ^{-5}]	ε	d_1[Å]	d_2[Å]	d[Å]
N4–O2						
HF/6-311G**	3.860	-39.426	0.137	0.571	0.613	1.184
HF/6-311++G**	3.848	-39.321	0.137	0.570	0.615	1.185
MP2/6-311G**	3.356	-23.506	0.119	0.580	0.643	1.222
B3LYP/6-311G**	3.420	-24.707	0.106	0.586	0.633	1.219
BLYP/6-311G**	3.236	-19.742	0.093	0.595	0.641	1.236
BP86/6-311G**	3.288	-21.085	0.095	0.590	0.640	1.231
N5–O3						
HF/6-311G**	3.892	-40.026	0.138	0.568	0.612	1.180
HF/6-311++G**	3.881	-39.959	0.139	0.568	0.613	1.181
MP2/6-311G**	3.385	-23.925	0.118	0.577	0.642	1.218
B3LYP/6-311G**	3.466	-25.602	0.104	0.582	0.631	1.213
BLYP/6-311G**	3.288	-20.739	0.090	0.590	0.640	1.229
BP86/6-311G**	3.336	-22.018	0.092	0.586	0.639	1.224
N5–O4						
HF/6-311G**	3.878	-39.787	0.136	0.569	0.613	1.182
HF/6-311++G**	3.866	-39.672	0.135	0.569	0.614	1.183
MP2/6-311G**	3.377	-23.851	0.116	0.577	0.642	1.219
B3LYP/6-311G**	3.456	-25.451	0.103	0.582	0.632	1.214
BLYP/6-311G**	3.280	-20.608	0.088	0.590	0.640	1.230
BP86/6-311G**	3.328	-21.887	0.091	0.586	0.639	1.225
N6–O5						
HF/6-311G**	3.892	-40.029	0.138	0.568	0.612	1.180
HF/6-311++G**	3.881	-39.955	0.139	0.568	0.613	1.181
MP2/6-311G**	3.384	-23.922	0.118	0.577	0.642	1.218
B3LYP/6-311G**	3.466	-25.605	0.104	0.582	0.631	1.213
BLYP/6-311G**	3.288	-20.737	0.090	0.590	0.640	1.229
BP86/6-311G**	3.336	-22.016	0.092	0.586	0.639	1.224
N6-O6						
HF/6-311G**	3.879	-39.802	0.136	0.569	0.613	1.182
HF/6-311++G**	3.866	-39.670	0.135	0.569	0.614	1.183
MP2/6-311G**	3.377	-23.858	0.116	0.577	0.642	1.219
B3LYP/6-311G**	3.456	-25.453	0.103	0.582	0.632	1.214
BLYP/6-311G**	3.280	-20.603	0.088	0.590	0.640	1.230
BP86/6-311G**	3.328	-21.882	0.091	0.586	0.639	1.225
C1-H1						
HF/6-311G**	2.001	-26.742	0.041	0.698	0.389	1.087
HF/6-311++G**	2.000	-26.721	0.041	0.698	0.389	1.087

Bonds	ρ [eÅ⁻³]	∇²ρ[eÅ⁻⁵]	ε	d_1[Å]	d_2[Å]	d[Å]
MP2/6-311G**	1.875	-22.792	0.031	0.715	0.386	1.101
B3LYP/6-311G**	1.895	-22.978	0.036	0.711	0.387	1.098
BLYP/6-311G**	1.850	-21.621	0.034	0.715	0.390	1.106
BP86/6-311G**	1.829	-21.231	0.034	0.720	0.388	1.108
Bonds	**ρ [eÅ⁻³]**	**∇²ρ[eÅ⁻⁵]**	**ε**	**d_1[Å]**	**d_2[Å]**	**d[Å]**
C1–H2						
HF/6-311G**	2.112	-30.172	0.018	0.715	0.354	1.069
HF/6-311++G**	2.107	-30.010	0.018	0.715	0.354	1.069
MP2/6-311G**	1.974	-25.636	0.015	0.724	0.360	1.084
B3LYP/6-311G**	1.991	-25.850	0.016	0.722	0.361	1.082
BLYP/6-311G**	1.946	-24.324	0.016	0.723	0.366	1.090
BP86/6-311G**	1.916	-23.775	0.016	0.729	0.364	1.094
C2–H3						
HF/6-311G**	2.098	-29.865	0.026	0.717	0.354	1.070
HF/6-311++G**	2.092	-29.683	0.027	0.717	0.354	1.071
MP2/6-311G**	1.960	-25.311	0.024	0.725	0.361	1.085
B3LYP/6-311G**	1.980	-25.616	0.023	0.723	0.360	1.084
BLYP/6-311G**	1.935	-24.080	0.023	0.725	0.366	1.091
BP86/6-311G**	1.904	-23.537	0.022	0.731	0.364	1.095
C2–H4						
HF/6-311G**	2.029	-27.517	0.048	0.698	0.383	1.081
HF/6-311++G**	2.027	-27.471	0.048	0.699	0.383	1.081
MP2/6-311G**	1.909	-23.738	0.039	0.713	0.380	1.093
B3LYP/6-311G**	1.923	-23.742	0.044	0.710	0.383	1.092
BLYP/6-311G**	1.877	-22.349	0.042	0.713	0.386	1.100
BP86/6-311G**	1.857	-21.971	0.042	0.718	0.384	1.102
C3–H5						
HF/6-311G**	2.001	-26.746	0.041	0.698	0.389	1.087
HF/6-311++G**	2.000	-26.720	0.041	0.698	0.389	1.087
MP2/6-311G**	1.875	-22.795	0.031	0.715	0.386	1.100
B3LYP/6-311G**	1.896	-22.986	0.036	0.711	0.387	1.098
BLYP/6-311G**	1.850	-21.621	0.034	0.716	0.390	1.106
BP86/6-311G**	1.830	-21.234	0.034	0.720	0.388	1.108
C3-H6						
HF/6-311G**	2.112	-37.522	0.018	0.715	0.354	1.069
HF/6-311++G**	2.107	-37.400	0.018	0.715	0.354	1.069
MP2/6-311G**	1.974	-33.159	0.015	0.724	0.360	1.084
B3LYP/6-311G**	1.991	-33.445	0.016	0.722	0.361	1.082

BLYP/6-311G**	1.946	-32.008	0.016	0.723	0.366	1.089
BP86/6-311G**	1.916	-31.354	0.016	0.729	0.364	1.094

Bonds	G(r)	V(r)	H(r)
C1–N1			
HF/6-311G**	1.375	-3.824	-2.450
HF/6-311++G**	1.363	-3.800	-2.436
MP2/6-311G**	0.898	-2.956	-2.058
B3LYP/6-311G**	0.803	-2.707	-1.904
BLYP/6-311G**	0.713	-2.391	-1.678
BP86/6-311G**	0.769	-2.557	-1.787
C2–N2			
HF/6-311G**	1.509	-4.026	-2.517
HF/6-311++G**	1.499	-4.004	-2.505
MP2/6-311G**	0.950	-3.068	-2.118
B3LYP/6-311G**	0.861	-2.850	-1.988
BLYP/6-311G**	0.759	-2.516	-1.757
BP86/6-311G**	0.816	-2.673	-1.857
C3–N3			
HF/6-311G**	1.557	-4.187	-2.631
HF/6-311++G**	1.551	-4.171	-2.620
MP2/6-311G**	0.995	-3.258	-2.263
B3LYP/6-311G**	0.900	-3.018	-2.118
BLYP/6-311G**	0.793	-2.684	-1.890
BP86/6-311G**	0.852	-2.838	-1.987
C1–N2			
HF/6-311G**	1.557	-4.188	-2.630
HF/6-311++G**	1.551	-4.171	-2.620
MP2/6-311G**	0.996	-3.259	-2.263
B3LYP/6-311G**	0.900	-3.019	-2.118
BLYP/6-311G**	0.793	-2.684	-1.891
BP86/6-311G**	0.852	-2.839	-1.987
C2–N3			
HF/6-311G**	1.507	-4.025	-2.518
HF/6-311++G**	1.499	-4.004	-2.505
MP2/6-311G**	0.950	-3.068	-2.118
B3LYP/6-311G**	0.862	-2.850	-1.989
BLYP/6-311G**	0.759	-2.516	-1.757
BP86/6-311G**	0.816	-2.673	-1.858
C3–N1			
HF/6-311G**	1.375	-3.824	-2.449
HF/6-311++G**	1.363	-3.799	-2.436
MP2/6-311G**	0.899	-2.957	-2.059

B3LYP/6-311G**	0.804	-2.708	-1.904
BLYP/6-311G**	0.713	-2.390	-1.677
BP86/6-311G**	0.769	-2.555	-1.786

Bonds	G(r)	V(r)	H(r)
N1–N4			
HF/6-311G**	1.166	-3.931	-2.766
HF/6-311++G**	1.162	-3.901	-2.739
MP2/6-311G**	1.153	-3.160	-2.007
B3LYP/6-311G**	1.100	-3.090	-1.991
BLYP/6-311G**	1.018	-2.618	-1.600
BP86/6-311G**	1.072	-2.809	-1.737
N2–N5			
HF/6-311G**	1.105	-3.696	-2.591
HF/6-311++G**	1.101	-3.668	-2.567
MP2/6-311G**	1.079	-2.895	-1.816
B3LYP/6-311G**	1.012	-2.751	-1.740
BLYP/6-311G**	0.918	-2.242	-1.324
BP86/6-311G**	0.974	-2.440	-1.467
N3–N6			
HF/6-311G**	1.104	-3.693	-2.589
HF/6-311++G**	1.101	-3.669	-2.567
MP2/6-311G**	1.079	-2.895	-1.815
B3LYP/6-311G**	1.012	-2.751	-1.739
BLYP/6-311G**	0.918	-2.243	-1.324
BP86/6-311G**	0.974	-2.441	-1.467
N4–O1			
HF/6-311G**	2.914	-8.587	-5.673
HF/6-311++G**	2.895	-8.543	-5.648
MP2/6-311G**	2.790	-7.224	-4.435
B3LYP/6-311G**	2.633	-6.996	-4.363
BLYP/6-311G**	2.495	-6.371	-3.876
BP86/6-311G**	2.561	-6.596	-4.035
N4–O2			
HF/6-311G**	2.914	-8.588	-5.674
HF/6-311++G**	2.895	-8.543	-5.648
MP2/6-311G**	2.790	-7.226	-4.436
B3LYP/6-311G**	2.633	-6.995	-4.363
BLYP/6-311G**	2.497	-6.375	-3.879
BP86/6-311G**	2.562	-6.600	-4.038
N5–O3			
HF/6-311G**	2.966	-8.734	-5.768
HF/6-311++G**	2.948	-8.694	-5.746

MP2/6-311G**	2.840	-7.356	-4.515
B3LYP/6-311G**	2.696	-7.185	-4.488
BLYP/6-311G**	2.565	-6.581	-4.016
BP86/6-311G**	2.627	-6.795	-4.168

Bonds	G(r)	V(r)	H(r)
N5–O4			
HF/6-311G**	2.946	-8.678	-5.732
HF/6-311++G**	2.927	-8.630	-5.704
MP2/6-311G**	2.830	-7.331	-4.500
B3LYP/6-311G**	2.685	-7.151	-4.467
BLYP/6-311G**	2.556	-6.555	-3.999
BP86/6-311G**	2.618	-6.768	-4.150
N6–O5			
HF/6-311G**	2.966	-8.734	-5.768
HF/6-311++G**	2.948	-8.693	-5.745
MP2/6-311G**	2.840	-7.355	-4.515
B3LYP/6-311G**	2.696	-7.185	-4.489
BLYP/6-311G**	2.565	-6.581	-4.016
BP86/6-311G**	2.626	-6.794	-4.168
N6–O6			
HF/6-311G**	2.947	-8.680	-5.733
HF/6-311++G**	2.927	-8.630	-5.704
MP2/6-311G**	2.831	-7.332	-4.501
B3LYP/6-311G**	2.685	-7.152	-4.467
BLYP/6-311G**	2.556	-6.554	-3.998
BP86/6-311G**	2.618	-6.767	-4.150
C1–H1			
HF/6-311G**	0.234	-2.341	-2.106
HF/6-311++G**	0.233	-2.336	-2.103
MP2/6-311G**	0.280	-2.156	-1.876
B3LYP/6-311G**	0.241	-2.090	-1.849
BLYP/6-311G**	0.241	-1.996	-1.755
BP86/6-311G**	0.238	-1.962	-1.724
C1–H2			
HF/6-311G**	0.186	-2.484	-2.298
HF/6-311++G**	0.184	-2.469	-2.285
MP2/6-311G**	0.248	-2.291	-2.043
B3LYP/6-311G**	0.204	-2.217	-2.013
BLYP/6-311G**	0.208	-2.119	-1.911
BP86/6-311G**	0.205	-2.074	-1.869
C2–H3			
HF/6-311G**	0.184	-2.458	-2.274

HF/6-311++G**	0.182	-2.442	-2.260
MP2/6-311G**	0.247	-2.266	-2.019
B3LYP/6-311G**	0.203	-2.200	-1.997
BLYP/6-311G**	0.208	-2.103	-1.894
BP86/6-311G**	0.205	-2.058	-1.853

Bonds	G(r)	V(r)	H(r)
C2–H4			
HF/6-311G**	0.228	-2.382	-2.154
HF/6-311++G**	0.226	-2.375	-2.149
MP2/6-311G**	0.275	-2.211	-1.936
B3LYP/6-311G**	0.237	-2.136	-1.899
BLYP/6-311G**	0.238	-2.040	-1.802
BP86/6-311G**	0.235	-2.008	-1.773
C3–H5			
HF/6-311G**	0.234	-2.341	-2.107
HF/6-311++G**	0.233	-2.336	-2.103
MP2/6-311G**	0.280	-2.156	-1.876
B3LYP/6-311G**	0.241	-2.091	-1.850
BLYP/6-311G**	0.241	-1.996	-1.755
BP86/6-311G**	0.238	-1.962	-1.724
C3–H6			
HF/6-311G**	0.186	-2.484	-2.298
HF/6-311++G**	0.184	-2.469	-2.285
MP2/6-311G**	0.248	-2.291	-2.043
B3LYP/6-311G**	0.204	-2.217	-2.013
BLYP/6-311G**	0.208	-2.120	-1.912
BP86/6-311G**	0.205	-2.074	-1.869

4. Energy Density

As an alternate for Laplacian of electron density, one can describe the chemical bonding in terms of local energy density H(r) then,

$$H(r) = G(r) + V(r)$$

where H(r) is total energy density, V(r) is a potential energy density, always negative and G(r) is kinetic energy density, always positive. Higher the dominance of V(r) in the bonding region, higher the charge accumulation and the G(r) reveals the depletion of charge density in the bonds. The energy density values for all the bonds of molecule were calculated from HF, MP2 as well as DFT theory. The energy densities of the adjacent C–N bonds in the ring are almost equal. The HF method predicts the potential energy density V(r) for the bonds C1–N2 and C3–N3 are almost equal and the average is ~4.2 H$\mathring{A}^{-3}$, and this value is much larger compared to MP2 and DFT methods, as their average values are ~3.3 and ~2.8 H$\mathring{A}^{-3}$ repectively. The similar trend exhibit in C2–N3, C2–N2 [~4.0, ~3.1 and ~2.7 H$\mathring{A}^{-3}$] and C3–N1, C1–N1 bonds [~3.8, ~3.0 and ~2.6 H$\mathring{A}^{-3}$] predicted by HF, MP2 and DFT levels of theory. Among all the bonds the N=O bonds possess maximum potential energy density V(r) which is invariably noticed in the three methods. Because of the higher charge accumulation in N=O, the potential energy density V(r) dominates well, the predicted average total energy density H(r) values are ~-5.7, ~4.5 and ~4.2 H.$\mathring{A}^{-3}$ respectively. Like C–N bonds, the local potential energy density V(r) for N–N bonds are higher in HF and found less in correlation methods. The HF method predicts a high negative potential energy density in N1–N4 bond its corresponding Laplacian values also high and these values are found decline in MP2 and DFT [Fig 5]. This large charge concentration in the bonding region attributes the maximum potential energy density V(r) [~-3.9 (HF), ~-3.2 (MP2) and ~2.8 (DFT) H.$\mathring{A}^{-3}$]. The total energy

density H(r) for N1–N4 bond are ~-2.8(HF), ~-2.0(MP2) and ~-1.8 HÅ^{-3}(DFT). These energy densities are larger than that of N3–N5 and N4–N6 bonds with an average H(r) [~-2.6(HF), ~-1.8(MP2) and ~-1.5 HÅ^{-3}]. These trends are clearly observed in Fig 5. On the whole, the minimum total energy density H(r) among all other bonds, calculated from high level of theory (BLYP), shows the weakness of N–N bonds of RDX explosive.
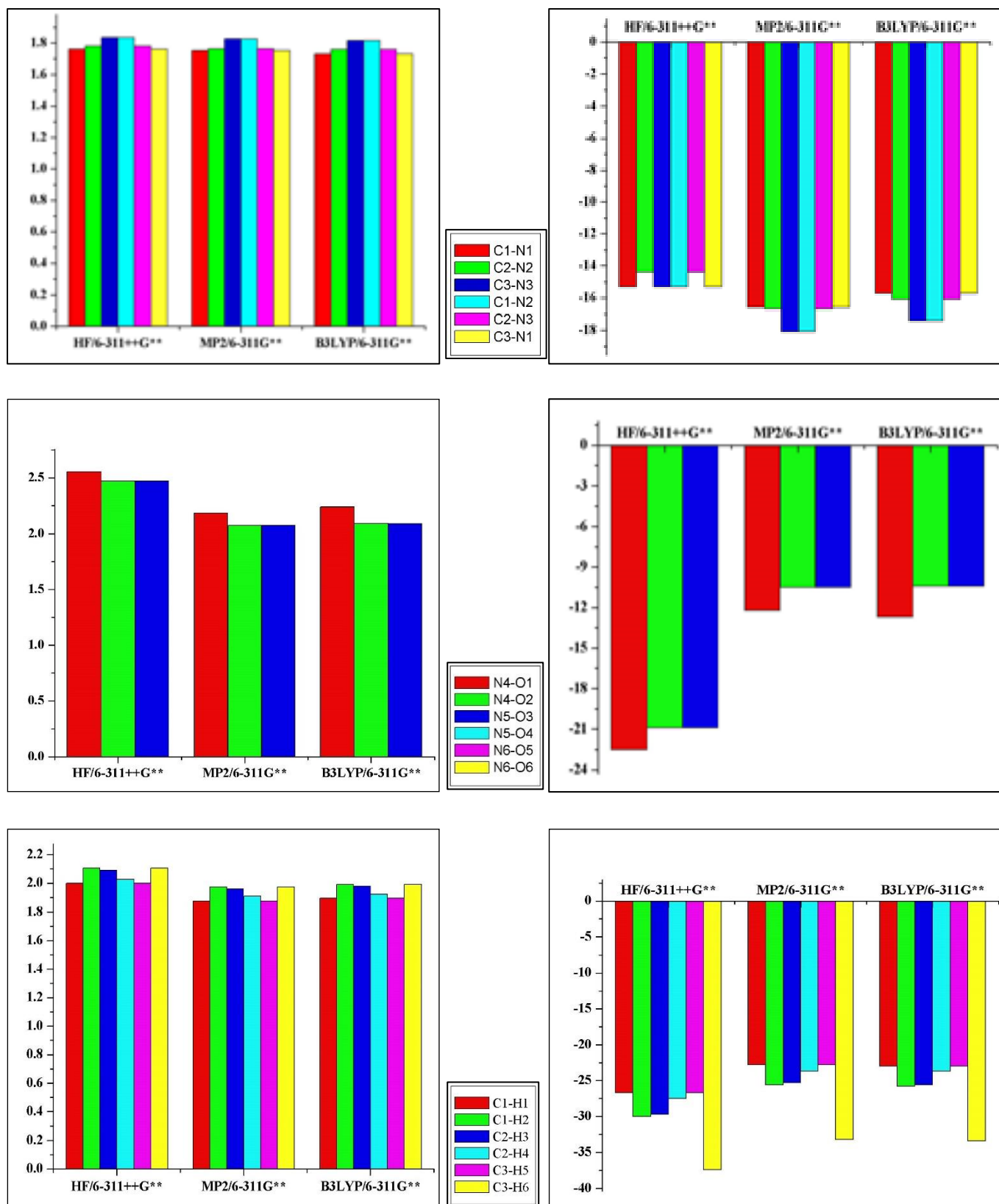

Fig 4. The electron density $\rho_{bcp}(r)$ and Laplacian of electron density $\nabla^2\rho_{bcp}(r)$ for HF, MP2 and DFT of RDX Molecule.
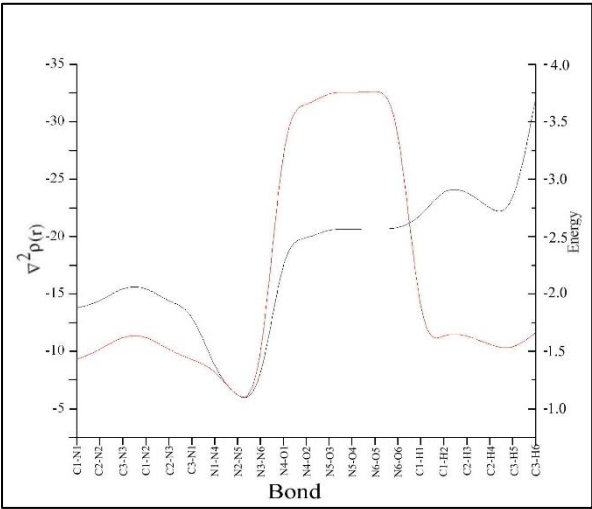
Fig 5. Laplacian of Electron density (black line) and total energy density (red line) calculated at BLYP level.

5. Atomic Charges

The NPA MPA, and CHELPG charges have been calculated (table 4) for MP2/6-311G** level and further the group charges of all NO_2 groups in the molecule are also calculated and the values are shown in Fig 6(a)-(c). From the NPA and MPA charge layouts, it was found that, the $-NO_2$ fragments bearing slightly negative charges (-0.08, -0.06, -0.06 e and -0.09, -0.07, -0.07 e) and the one for N1, N2 and N3 atoms having highly negative charges, lead no hyperconjugation of the molecule. Going to CHELPG charge layouts, the charge distribution becomes totally different. The CHELPG charges for $-NO_2$ fragments attached at N1, N2 and N3 atoms are -0.04, +0.08 and +0.08 e respectively. The corresponding charge for N1, N2 and N3 atoms are -0.24, -0.47 and -0.47 e respectively. This leads to strong hyperconjugation effect in the molecule and make N–N bonds be highly polarized, especially N2–N5 and N3–N6 bonds, as $N2^{\delta-}-NO_2^{\delta+}$ and $N3^{\delta-}-NO_2^{\delta+}$ respectively, which confirms the weakness of N–N bonds in the molecule.

Table IV. Atomic charges (e) [NPA, MPA and CHELPG] of RDX molecule calculated at MP2 level.

Atom	NPA	MPA	CHELPG
C1	-0.02	0.02	0.11
C2	-0.02	-0.01	0.21
C3	-0.02	0.02	0.11
N1	-0.36	-0.31	-0.24
N2	-0.36	-0.29	-0.47
N3	-0.36	-0.29	-0.47
N4	0.62	0.41	0.68
N5	0.61	0.4	0.8
N6	0.61	0.4	0.8
O1	-0.35	-0.25	-0.36
O2	-0.35	-0.25	-0.36
O3	-0.33	-0.23	-0.35
O4	-0.34	-0.24	-0.37
O5	-0.33	-0.23	-0.35
O6	-0.34	-0.24	-0.37
H1	0.18	0.16	0.09
H2	0.25	0.2	0.14
H3	0.26	0.22	0.11
H4	0.21	0.18	0.1
H5	0.18	0.16	0.09
H6	0.25	0.2	0.14

6. Electrostatic Potential

The molecular electrostatic potential (MEP) calculations have been done to predict the polarization, electron correlation and charge transfer effects within the molecule. Fig 7 shows the theoretical MEP obtained from MP2 level of calculation as negative (red) and positive (blue) regions of the property at the +0.5 eÅ-1 and -0.05 eÅ-1 isosurface value. The polarization nature of N–NO2 fragments in RDX and the hypercojugation effect of N–N bonds in the molecule was quite clear (Fig 7), the negative regions are concentrated around the oxygen atoms, while the rest of the molecule has positive ESP. In this iso-surface we noticed one surface of the molecule highly electronegative region and the other surface mounted with positive. This dominant electronegative region may be important for the RDX's extra-ordinary less impact sensitivity compare with other explosive materials.
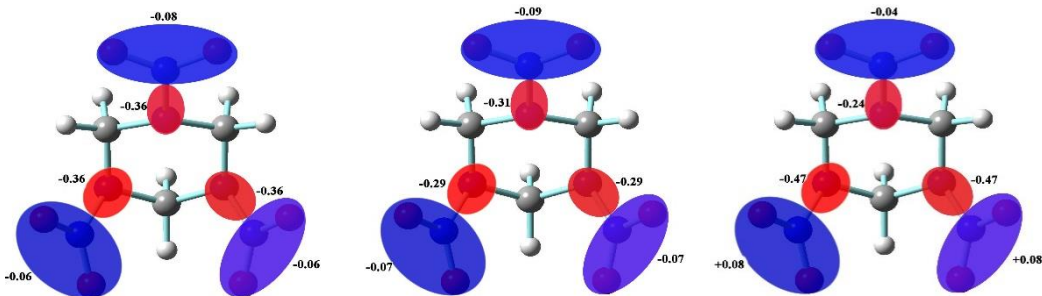

Fig 6. Group charge layouts of N–NO$_2$ fragments (a)NPA (b) MPA (c) CHELPG
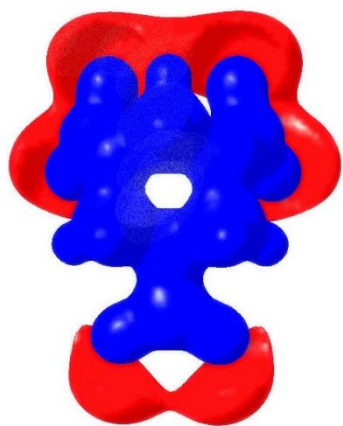
Fig 7. The isosurface representation of Electrostatic potential of RDX molecule. Blue: positive ($+0.5$ eÅ^{-1}), red: negative potential (-0.05 eÅ^{-1}).

Conclusion

Depending upon the various ab initio and DFT levels of calculations, the N–N bond length varies significantly, and obtain higher values, when the electron correlation effect is included. N1–N4 bond length is shorter than N2–N5 and N3–N6 bonds for all level of calculations. The shorter N1–N4 bond, have high electron density and significant charge concentration at the bond critical point. On the other hand, the $\square$bcp(r) in N2–N5 and N3–N6 bonds are found lesser and the charges are more depleted. This ensures that, predicting the geometric features accurately is of considerable importance in determining the bond properties. This was obvious from energy density calculation, as the N–N bonds have the minimum total energy density H(r) obtained from DFT level of theory. Finally, weakness of N–N bonds, again pointed out from hyperconjugation effect, as N2δ-–NO2δ+ and N3δ-–NO2δ+ respectively, recommended from CHELPG charge and MEP analysis. On the whole, we conclude that the N–N bonds, especially, N2–N5 and N3–N6 are the weakest bonds of RDX energetic molecule.

References

1. A.K Sikder and Nirmala Sikder, A review of advanced high performance, insensitive and thermally stable energetic materials emerging for military and space applications, *J. Hazard. Mater,* 112(2004) 1-15.

2. S. P. Gejji, M. B. Talawar, T. Mukundan , E. M. Kurian, Quantum chemical, ballistic and explosivity calculations on 2,4,6,8-tetranitro-1,3,5,7-tetraaza cyclooctatetraene: A new high energy molecule, J. Hazard,Mat, 36 (2006) A134.

3. S. F. Coffey, Phonon generation and energy localization by moving edge dislocations, Phys Rev, 24(1981) 6984-6990.

4. A. B. Kunz and D. R. Beck, Possible role of charged defects in molecular solids, Phys, Rev, B36 (1987) 7580-7585.

5. S. Zeman, Analysis and prediction of the Arrhenius parameters of low-temperature thermolysis of nitramines by means of the ^{15}N NMR spectroscopy, Thermochim. Acta, 121 (1999) 333.

6. G. A. Olah, D. R. Squire, Chemistry of Energetic Materials, *Academic Press*, San Diego (1991).

7. S. Borman, Advanced energetic materials emerge for military and space applications, Chem, Eng, News, 72 (1994) 18.

8. S. Zeman, Some predictions in the field of the physical thermal stability of nitramines, Thermochim, Acta, 302 (1997) 11.

9. A. K. Sikder, G. Maddala, J. P. Agraval and H. Singh, Important aspects of behaviour of organic energetic compounds: a review, *J. Hazard, Mater*, 84(2001) 1-26.

10. K. Y. Lee , M. D. Coburn, 3-nitro-1,2,4—triazol-5-one, a less sensitive explosive, Los. Alamos. Report LA-10302-MS, (1985).

11. K. Y. Lee, L. B. Chapman and M. D. Coburn, 3-Nitro-1,2,4-triazol-5-one, a less sensitive explosive, *J. Energ, Mater*, 5 (1987) 27-33.

12. S. J. Smith , B. T. Sutcliffe, The development of Computational Chemistry in the United Kingdom, Reviews in Computational Chemistry, 10 (1997) 271.

13. J. K. Labanowski, J. W. Andzelm, (Eds), Density Functional Methods in Chemistry. Springer, New York, (1991).

14. R. G. Parr , W. Yang, Density Functional Theory of Atoms and Molecules, Oxford, New York, (1989).

15. F. W. Biegler-Konig, R. F. W. Bader and T. J. Ting-Hau, Calculation of the average properties of atoms in molecules. II, *J. Comput. Chem*, 3(1982) 317-328.

16. R. F. W. Bader, Atoms in Molecules, A Quantum Theory, Clarendon Press, Oxford (1990).

17. C. Dieter , E. Kraka, A Description of the Chemical Bond in Terms of Local Properties of Electron Density and Energy, *Croatica Chemica Acta*, 57 (1984) 1259-1281.

18. D. V. Korol'kov, Virial theorem and the chemical bond phenomenon, *J. Struct. Chem,* 33 (1992) 335- 342.

19. M. J. Frisch, G. W. Trucks, H. B. Schlegel, G. E. Scuseria, M. A. Robb, J. R. Cheeseman, J. A. Montgomery, Jr. Vreven, K. N. Kudin, J. C. Burant, J. M. Millam, S. S. Iyengar, J. Tomasi, V. Barone, B. Mennucci, M. Cossi, G. Scalmani, N. Rega, G. A. Petersson, H. Nakatsuji, M. Hada, M. P. Ehara, K. Toyota, R. Fukuda, J. Hasegawa, M. Ishida, T. Nakajima, Y. Honda, O. Kitao, H. Nakai, M. Klene, X. Li, J. E. Knox, H. P. Hratchian, J. B. Cross, Adamo, J. Jaramillo, R. Gomperts, R. E. Stratmann, O. Yazyev, A. J. Austin, R. Cammi, C. Pomelli, J. W. Ochterski, P. Y. Ayala, Morokuma, G. A. Voth, P. Salvador, J. J. Dannenberg, V. G. Zakrzewski, S. Dapprich, A. D. Daniels, M. C. Strain, O. Farkas, D. K. Malick, A. D. Rabuck, K. Raghavachari, J. B. Foresman, J. V. Ortiz, Q. Cui, A. G. Baboul, S. Clifford, J. Cioslowski, B. B. Stefanov, G. Liu, A. Liashenko, P. Piskorz, I. Komaromi, R. L. Martin, D. J. Fox, T. Keith, M. A. Al-Laham, C. Y. Peng, A.

Nanayakkara, M. Challacombe, P. M. W. Gill, B. Johnson, W. Chen, M. W. Wong, C. Gonzalez , J. A. Pople, Gaussian, Inc., Pittsburgh PA, (2003).

20. A. R. Leech, Molecular Modelling, Longman, Essex, (1997).

21. M. J. Frisch, M. Head-Gordon J. A. Pople, A direct MP2 gradient method, *Chem. Phys, Lett*, 166 (1990) 275-280.

22. R. G. Parr, W. Yang. Density Functional Theory of Atoms and Molecules, Oxford University Press, London, (1989).

23. C. Lee, W. Yang and R. G. Parr, Development of the Colle-Salvetti correlation-energy formula into a functional of the electron density, *Phy, Rev,* B37(1998) 785-789.

24. J. P. Perdew, Density-functional approximation for the correlation energy of the inhomogeneous electron gas, *Phys Rev,* B33 (1986) 8822-8824.

25. J. Cheeseman, T. A. Keith , R. F. W. Bader, AIMPAC Program Package McMaster University Hamilton, Ontario (1992).

26. T. Koritsanszky, P. Macchi, C. Gatti, L. J. Farrugia, P. R. Mallinson, A. Volkov and T. Richter, XD-2006. A Computer Program Package for Multipole Refinement and Topological Analysis of Charge Densities and Evaluation of Intermolecular Energies from Experimental or Theoretical Structure Factors, Version 5, 33 (2007).

27. C. S. Choi and E. Prince, The crystal structure of cyclotrimethylenetrinitramine, *Acta Cryst*, B28 (1972) 2857-2862.

About The License